Photochemical mineralization of dissolved organic nitrogen to ammonia in prairie lakes

4 AUTHORS, INCLUDING:

Jeff Sereda
University of Saskatchewan
15 PUBLICATIONS **142** CITATIONS

SEE PROFILE

Kristine Hunter
University of Saskatchewan
3 PUBLICATIONS **18** CITATIONS

SEE PROFILE

PRIMARY RESEARCH PAPER

Photochemical mineralization of dissolved organic nitrogen to ammonia in prairie lakes

Sereda Jeff · Kristine Hunter ·
David Vandergucht · Jeff Hudson

Abstract We examined the rate of photoammonification in 16 lakes from Saskatchewan, Canada. Lakes were selected to encompass a broad range in dissolved organic nitrogen (DON) (269–1,435 µg l^{-1}). Lake filtrate (<0.2 µm) was exposed to artificial solar radiation for 4 h. Rates of photoammonification were significant in 7 of the 16 study lakes. Ammonia (NH$_3$) concentrations increased 0.84–2.85 µg l^{-1} over control values. This is a 4–92% increase in NH$_3$ concentration and a conversion of 0.18–0.3% of the DON pool to NH$_3$. We developed an empirical model to predict photoammonification rates across aquatic ecosystems. Photoammonification rates and ancillary parameters (i.e., pH, DOC and DON concentrations, DOC:DON ratios, and a350:DOC) were obtained from published studies to expand our dataset for model development. Model selection was conducted with Akaike's Information Criterion (AIC). DON concentration and pH were selected as model predictors by AIC. Our model explains 49% of the variance in photoammonification rate across a diverse set of aquatic systems. This model may be useful in estimating photoammonification rates in other aquatic systems.

Introduction

The release of ammonium from the photochemical degradation of dissolved organic matter (DOM) may be a potentially important remineralization pathway for refractory dissolved organic nitrogen (DON) (Bushaw et al., 1996; Wang et al., 2000; Koopmans & Bronk, 2002). Photoammonification has been demonstrated in marine and estuarine systems (Bushaw et al., 1996; Gardner et al., 1998; Bushaw-Newton & Moran, 1999; Morell & Corredor, 2001; Koopmans & Bronk, 2002; Buffam & McGlathery, 2003), freshwater rivers, wetlands, and ponds (Bertilsson et al., 1999; Grzybowski, 2002), but little information on rates of photoammonification in freshwater lakes is available. Lakes within the Interior Plains of North America are often N limited (Prepas & Trimbee, 1988; Salm et al., 2009). The DON fraction often exceeds 50% of the total dissolved N (TDN) pool in freshwaters (Krupka, 1989; Wetzel, 2001). Photoammonification may represent a significant pathway supplying NH$_3$ to primary producers (PP) and further investigation is warranted.

S. Jeff (✉) · K. Hunter · D. Vandergucht · J. Hudson
University of Saskatchewan, 112 Science Place,
WP Thompson Building, Saskatoon, SK S7N 5E2,
Canada
e-mail: jeff.sereda@usask.ca

Rates of photoammonification reported across studies have been inconsistent. For example, photoammonification rates of up to 220 and 4,700 nmol l^{-1} h^{-1} have been observed in salt (Gardner et al., 1998) and fresh water (Wang et al., 2000), respectively, whereas, several studies have been unable to detect significant levels of photoammonification in lake and river water (Jørgensen et al., 1998; Bertilsson et al., 1999; Wiegner & Seitzinger, 2001). These contrasting observations likely reflect regional variability in DOM reactivity (e.g., autochthonous vs. allochthonous DOM), and the effects of various environmental controls [e.g., iron (Fe), potential hydrogen ion concentration (pH), and ambient ammonia (NH_3) concentrations]. For example, photoammonification rates tend to be greater in waters with high concentrations of iron (Fe) (Gao & Zepp, 1998) and low pH (Wang et al., 2000) because photofenton reactions accelerate photodegradation processes (Zepp et al., 1992; White et al., 2003). Whereas, in systems with high ambient NH_3 concentrations a net decrease in NH_3 concentration may occur through the photochemical-mediated loss of NH_3 (Koopmans & Bronk, 2002).

Photoammonification rates may also depend on the composition of DOM. Daily areal photoammonification rates may be 4–6 times greater at sites where DOM is dominated by autochthonous rather than allochthonous production (Stedmon et al., 2007). This is likely related to terrestrial (allochthonous) DOM generally being N poor (i.e., high DOC:DON ratio) (Benner, 2002; Bronk & Ward, 2002; Stepanauskas et al., 2002). Photoammonification rates may, therefore, increase with increasing DON concentrations.

Freshwaters generally exhibit higher rates of photoammonification compared to estuarine and marine systems (Kitidis et al., 2006, p. 445, Table 3). Higher concentrations of chromophoric DOM (CDOM) present in freshwater compared to saline environments may account for this variation. Photoammonification rates should be greater from more intensely colored DOM, as photobleaching (i.e., loss of DOM color) decreases DOM photoreactivity. For example, the greatest rates of photoammonification in a boreal pond were observed in irradiated water collected shortly after spring thaw (Bushaw et al., 1996). Kitidis et al. (2006) observed that photoammonification rates were significantly correlated with CDOM concentrations (as measured by absorbance at 300 nm normalized to DOC), and that photochemical

NH_3 production decreased as photobleaching progressed. These results suggest that photoammonification may be greatest for CDOM with little prior exposure to sunlight (Bushaw et al., 1996). Differences in CDOM:DOC ratios may be of value for inferring photoammonification rates across systems (Kitidis et al., 2006).

Rates of photoammonification have been correlated with pH, CDOM and NH_3 concentrations, light exposure history of DOM, and the rate of autochthonous versus allochthonous DOM production (i.e., DOC:DON ratios). Each of these factors will vary seasonally and geographically. Photoammonification rates must, therefore, be considered in their seasonal and regional context. Primary productivity is frequently N limited within lakes of the Interior Plains of North America (Prepas & Trimbee, 1988; Salm et al., 2009). DON often comprises >75% of the dissolved N pool in Interior Plain lakes (Sereda & Vandergucht, unpublished data) and the photochemical liberation of NH_3 from DON may be a significant pathway supplying N to PPs. Lakes within the Interior Plains are typically alkaline, with high concentrations of colorless DOC (Sereda et al., 2011). These lakes are an interesting contrast to the highly colored, acidic, inland waters that have been studied previously (Bushaw et al., 1996; Bertilsson et al., 1999; Wang et al., 2000). Therefore, our study had several objectives. First, to determine if photoammonification was detectable in 16 freshwater, alkaline, low CDOM lakes by exposing lake filtrate to simulated solar radiation. Second, we compared our rates of photoammonification with rates observed in other studies. Third, we determined which water chemistry parameters best predict rates of photoammonification (e.g., pH, DON, DOC, ambient NH_3 and/or CDOM concentrations) in our study lakes. And finally, we expanded our dataset with measurements of photoammonification from published studies and develop a model for predicting photoammonification rate in relation to water chemistry.

Materials and methods

We sampled 16 freshwater polymictic (i.e., isothermal) lakes during August and September, 2010 located in Saskatchewan, Canada. Mixing of the water column

was confirmed through vertical profiles of temperature, dissolved oxygen, pH, and total dissolved solids obtained with a single sonde cast (YSI 6600 multi parameter sonde). These measures were homogeneous from the top to the bottom of study lakes indicating that lakes were well mixed. Lakes were selected to encompass a broad range of TDN, DON, NH_3, and DOC (Table 1). Sampling was restricted to approximately a 1-month period to minimize variability in lake response to UVR treatment that may result from inter- and intra-seasonal differences in environmental conditions (e.g., in situ solar radiation, influxes of DOC, DON etc.).

Surface lake water (~ 20 l, discrete samples) was collected 1 m below the surface with a Van Dorn sampler. Water was gently decanted into a collapsible polyethylene bag that had been washed (0.1% Liqui-Nox P-free detergent), leached (dilute HCl), and rinsed with lake water. Water samples were transported to the laboratory in a cooler at ambient lake temperature within 4 h of collection.

Total nitrogen (TN) and nitrate (NO_3^-) concentrations were determined using second derivative spectroscopy (Crumpton et al., 1992; Bachmann & Canfield, 1996). Ammonia concentration was determined colorimetrically with the phenol–hypochlorite technique according to Stainton et al. (1974). DON was determined through subtraction [TN—total inorganic N (NO_3, NH_3)]. DOC concentration was measured on a Shimadzu total organic carbon analyzer (TOC-5050A). Chlorophyll a (chl a) samples were collected under low light conditions on 47 mm GF/F (1–2 l, vacuum filtration 10 psi). Chlorophyll pigments were extracted in the dark and analyzed according to Bergmann & Peters (1980) with the following changes; absorbance was read at 665 nm rather than 655 nm, and chl a samples were left in 95% ethanol for 24 h in the dark at room temperature rather than refrigerated (Arvola, 1981).

Measurements of photoammonification

Lake filtrate (<0.2 μm, ~ 500 ml) was collected within 12 h of lake water collection through gentle syringe filtration (polycarbonate filter, Poretics, 47 mm). Borosilicate tubes (70 ml) (herein after referred to as incubation vessels) were filled completely with lake filtrate (i.e., no head space remained) and capped. Two treatments were established,

exposure to ultraviolet radiation (UVR) and photosynthetically active radiation (PAR) (herein after UVR treatment) and control ($n = 3$ for each). Controls were wrapped in aluminum foil and received no UVR or PAR irradiance. An additional three incubation vessels were filled with deionized water and treated identically to other incubation vessels to monitor for possible NH_3 contamination. Incubation vessels were then placed in a solar simulator (SunTest XLS+, Xenon lamp with a Suprax Daylight Glass Filter—290 nm cutoff, Atlas) and incubated for 4 h. Vessels were placed in a constant flow water bath to maintain ambient lake temperature ($\sim 20°C$). Measurements of simulated solar irradiance (W m^2) were measured at 0.5 nm wave lengths throughout the UVR (290–399 nm) and PAR (400–700 nm) spectrum with an Ocean Optics USB 2000 radiometer. Measurements were obtained with and without a borosilicate tube to determine filtering effects of the borosilicate. Total irradiance emitted by the solar simulator was 261 W m^{-2}; whereas, total irradiance in UVR treatment vessels was 256 W m^{-2}. The borosilicate tube permitted 99, 95, and 90% transmission of the PAR, UVA, and UVB radiation, respectively (Fig. 1). Output from the solar simulator was comparable to ambient natural UVR conditions observed in Saskatoon, SK (Sereda et al., unpublished data) (Fig. 1). At the end of the incubation, vessels were removed from the solar simulator and subsampled (50 ml) for NH_3 determination as described above. Photoammonification was calculated as the difference between NH_3 concentration in treatment vessels minus ambient NH_3 concentration in the lake water and the blanks.

Comparison of photoammonification rates

Photoammonification rates were obtained from the literature for a diversity of aquatic systems (Table 2) and compared to the rates we observed in this study. Environmental variables that were available for the greatest number of studies and are known to correlate with photoammonification rates [i.e., DOC, DON, DOC:DON ratios, DOM absorbance (i.e., a350:DOC), and pH] were also collected (Table 2).

Characterization of DOC

Absorption coefficients at 300 nm normalized for DOC concentration (i.e., a300:DOC) ψ have been

Table 1 Physical and chemical characteristics of the study lakes: depth (at sampling location), pH (note pH values are typically alkaline), chlorophyll a (Chl a), dissolved organic carbon (DOC), total dissolved N (TDN), dissolved organic nitrogen (DON), ambient ammonia (NH$_3$), a300 before (a300^1) and after (a300^2) UVR treatment, and a300:DOC ratios

| Lake	Latitude (N°)	Longitude (W°)	Depth (m)	pH	Chl a (µg l^{-1})	DOC (mg l^{-1})	TDN (µg l^{-1})	DON (µg l^{-1})	NH$_3$ (µg l^{-1})	a300^1 (m^{-1})	a300^2 (m^{-1})	a300:DOC (m^{-1} mg^{-1} l^{-1})
Athapapuskow	54°40'	101°40'	30	7.9	1.7	6.1	360	318	10.3	5.1	5.3	0.83
Heritage	53°55'	105°09'	13	8.4	3.8	9.3	532	467	3.9	7.0	6.8	0.78
Huard	53°48'	107°35'	3	8.4	19.1	18.4	1,066	893	6.0	21.2	19.1	1.15
Lower Blackstrap	51°48'	106°23'	7	8.3	20.6	7.5	643	570	4.6	8.9	8.4	1.19
Meewasin Pond	52°08'	106°38'	1	nd	27.5	23.3	1,669	1,434	8.4	78.5	73.6	3.37
Murray	53°02'	108°17'	6	8.7	11.4	12.1	999	829	6.7	19.3	27.0	1.59
Namekus	53°49'	106°01'	nd	nd	nd	11.1	798	595	6.4	14.1	12.7	1.28
Whiteswan	54°02'	105°08'	20	8.4	0.9	6.6	463	399	4.3	2.3	3.2	0.35
Miko	53°53'	107°43'	11	nd	3.4	9.3	332	268	4.1	10.8	10.3	1.16
Lower Emma	53°35'	105°53'	8	8.6	12.7	21.1	1,285	1,040	32.3	6.3	5.6	0.30
Middle Emma	53°37'	105°55'	7	8.4	9.5	22.4	1,403	1,135	56.7	10.4	9.9	0.47
Amisk	54°39'	102°07'	20	8.2	4.1	8	368	330	14.9	13.9	12.7	1.74
Bradwell	51°55'	106°11'	5	8.3	3.7	8.5	1,383	1,180	193.4	14.2	14.4	1.67
Bug	53°54'	107°44'	4	7.9	6.3	17.4	398	328	5.7	13.5	13.1	0.78
Upper Blackstrap	51°46'	106°27'	7	8.3	23.4	7.9	631	551	10.4	10.8	10.1	1.37
Zelma	51°49'	105°49'	6	8.3	3.4	14.4	1,686	1,231	235.6	19.3	18.0	1.34

nd no data
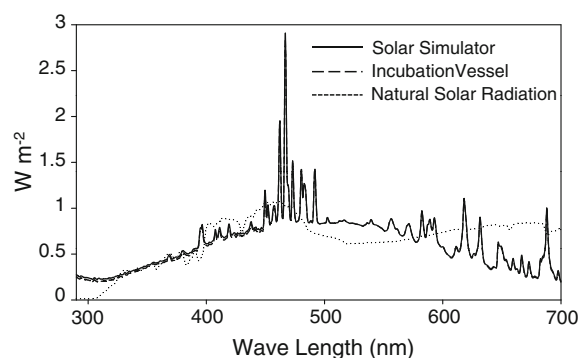
Fig. 1 Measurements of solar irradiance (W m^2) measured at 0.5 nm wave lengths throughout the UVR (290–399 nm) and PAR (400–700 nm) spectrum with an Ocean Optics USB 2000 radiometer. Measurements were obtained for our solar simulator (SunTest XLS+, Xenon lamp with a Suprax Daylight Glass Filter—290 nm cutoff, Atlas) with and without a borosilicate incubation vessel to determine filtering effects of the borosilicate. Also shown is ambient noon time solar irradiance observed during the summer in Saskatoon, SK (Sereda et al., unpublished data)

used as a proxies for CDOM concentration. Therefore, a300:DOC ratios were calculated for each lake. DOM absorbance was measured on a Shimadzu UV–Vis spectrophotometer (UV-2401) in a 10-cm quartz cuvette. The absorbance coefficient was calculated

[e.g., absorbance at 300 nm × 2.303/pathlength (m)] and normalized to DOC concentration (mg l^{-1}).

Across studies, there is considerable variation in the wavelength at which DOM absorbance is measured (e.g., a280, a300, a350, a365). Absorbance at 350 nm was most frequently reported (Table 1 of Grzybowski, 2003). Therefore, we also measured a350:DOC on our study lakes to have data complimentary to what was available for other studies to use in model development (Table 2).

Statistical analysis

Treatment effect on the photoammonification was determined with one-way analysis of variance (one-way ANOVA). Relationships between the photoammonification (μg l^{-1}) and water chemistry [i.e., pH, DOC, TDN, DON, NH$_3$ concentrations, DOC:DON ratios, and a300:DOC] were analyzed with linear regression. We selected linear models as linear relationships between photoammonification and pH, and a300/DOC (m^{-1} μmol^{-1} l) have been previously reported (Wang et al., 2000; Kitidis et al., 2006).

We then determined if a predictive model of photoammonification could be developed to estimate rates of photoammonification in relation to water

Table 2 A comparison of photoammonification rates observed in our study with rates reported in other published studies. Ancillary variables [pH, dissolved organic carbon (DOC), dissolved organic nitrogen (DON), and DOM absorbance (a350:DOC)] known to influence photoammonification rates have been included. Experimental conditions for each study have been summarized in Table 1 of Grzybowski (2003)

Study	System	pH	DOC (mg l^{-1})	DON (μg l^{-1})	a350:DOC	Photoammonification (μg l^{-1} h^{-1})
This study	Freshwater lakes	8.3 (mean)	12.7 (mean)	723.3 (mean)	0.03–0.65	0.25 (mean)
Bushaw et al. (1996)	Boreal Pond	7.6	36	770	1.19	2.04
	Okefenokee Swamp	3.9	46.1	1,204	2.29	2.97
	Suwanee River	nd	nd	1,036	nd	6.48
Wang et al. (2000)	Pearl River	6	29.9	340.2	1.10	5.94
	Bayou Trepagnier (1997)	6.6	8.1	1352.4	nd	21.6
	Bayou Trepagnier (1999)	6.4	27.3	1006.6	nd	34.2
	Bayou Trepagnier	6.6	6	1163.4	nd	30.6
	Bayou Trepagnier	8.1	712	nd	nd	84.6
Gao & Zepp (1998)	Satilla River	nd	25.2	nd	nd	1.8
Koopmans & Bronk (2002)	Town Creek	nd	nd	168	nd	4.32
Vahatalo et al. (2003)	Lake Valkea-Kotinen	5.1	10.081	356	nd	4.46

nd no data

chemistry across systems. We applied multiple linear regression using DOC and DON concentrations, DOC:DON ratios, pH, and a350:DOC (a proxy for CDOM concentration) as model predictors. DON and DOC:DON ratios were log-transformed to normalize variance (Zar, 1999). Photoammonification rates were $\log(x + 1)$ transformed to accommodate zero values in the analysis. pH and a350:DOC were not transformed. We used Akaike's Information Criterion (AIC) to select the most parsimonious model among candidate models containing the null (intercept only), single-predictor (e.g., either DOC, DON, DOC:DON ratios, a350:DOC, or pH), and two- to five-predictor equations (Burnham & Anderson, 2004). AIC is defined as: $-2(\text{log-likelihood}) + 2k$, where k is the number of estimable parameters of the model in question. We ranked models according to the distance in AIC units of each model relative to the best model ($\Delta \text{AIC} = \text{AIC}_i - \min \text{AIC}$, where AIC_i is the value for model i, and the min AIC is the value of the best model). Here, $\Delta \text{AIC} < 2$ gives support for a candidate model; whereas, ΔAIC values between 3 and 7 provide considerably less support, and $\Delta \text{AIC} > 10$ indicates that the model is improbable (Burnham & Anderson, 2004). Tolerance (a measure of collinearity between independent variables) was 0.99. Treatments were deemed statistically significant at an alpha level of 0.05. Statistical analyses were performed with Statistica v. 6.1 (StatSoft, Inc., Tulsa, Oklahoma).

Results

Water chemistry

Study lakes encompassed a broad range in DON (268.4–1,434.9 µg l^{-1}) and ambient NH$_3$ (1.05–235.6 µg l^{-1}) concentrations (Table 1). All study lakes were alkaline with a mean (± 1 standard deviation, SD) pH of 8.3 ± 0.2 (Table 1). DOC concentrations also varied considerably among study lakes (6.1–23.3 mg l^{-1}). The DOC pool was generally colorless (i.e., low absorbance values, Table 1).

Photoammonification

Ammonia concentrations increased significantly in 7 of the 16 study lakes with UV treatment (increases of 0.72–2.85 µg l^{-1}) (Fig. 2). This corresponds to a

conversion of 0.18–0.30% of the DON pool to ammonia and a 4–92% increase in ambient NH$_3$ concentration. Ammonia concentration increased in an additional 4 study lakes treated with UV, but the increase was not significant ($P > 0.05$, Fig. 2). A change in ammonia concentration was not observed in treatment vessels for the remaining 5 study lakes. In comparison, photoammonification rates across other published studies had a range of 1.8–84.6 µg l^{-1} h^{-1} and were considerably greater than the rates observed in this study (Table 2).

Relationship between photoammonification and water chemistry

A weak relationship between photoammonification and DON concentration was observed ($R^2 = 0.23$, $P = 0.06$, $n = 16$) (Fig. 3). A relationship between photoammonification, DOC and ambient NH$_3$ concentrations, DOC:DON ratios, pH, and a300:DOC was not observed ($R^2 \leq 0.51$, $P \geq 0.08$, $n = 16$).

Photoammonification rate and water chemistry parameters were available for a total 22 systems (including lakes in our study) for model development. Three of our study lakes were not included in the
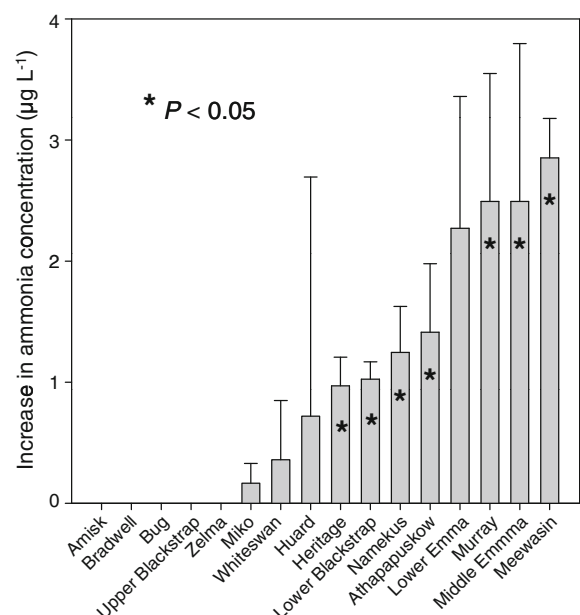

Fig. 2 Shown is the increase in ammonia concentration in treatment vessels following UVR treatment. Lakes are ordered (*left to right*) from no change to the greatest increase in NH$_3$ concentration. *Error bars* represent 1 standard deviation
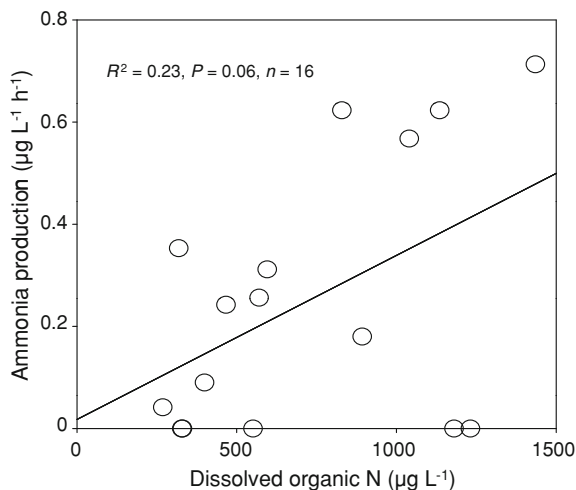
Fig. 3 Shown is the relationship between photoammonification rate and DON concentration

analysis because pH values were unavailable. The range of parameters used in model were broad; photoammonification (0–34 $\mu g \, l^{-1} \, h^{-1}$), pH (3.9–8.7), DOC (6–46 $mg \, l^{-1}$), DON (280–1,352 $\mu g \, l^{-1}$), DOC:DON (5–88), and a350:DOC (0.03–2.29) (Table 2). a350:DOC values were only available for an additional 3 studies (Table 2). Therefore, our initial model was developed using our study lakes and these 3 additional studies. a350:DOC was not a significant predictor of photoammonification ($P = 0.93$) based on model selection using AIC. Therefore, we re-developed our model using a larger set of systems ($n = 22$) for which

measurements of DOC, DON, DOC:DON ratios, and pH were available. We present only partial additive models (i.e., intercept plus DON and/or DOC concentration and pH as model predictors, Table 3) based on model selection using AIC. The partial models (DON concentration and pH) for predicting photoammonification rate were superior to the next-best model (DON + pH + DOC) by only 1.5 AIC units. Inclusion of DOC concentration in the model increased predictive power slightly (increase in R^2 from 0.49 to 0.51) (Table 3) although, the coefficient for DOC was non-significant ($P = 0.33$). DOC:DON was not a significant predictor of photoammonification ($P = 0.14$). DON concentration and pH were positively and negatively related to photoammonification rate, respectively (Table 3). DON concentration and pH explained 49% of the variation in photoammonification rate across systems ($R^2 = 0.49$, $P = 0.001$, $n = 22$). DON concentration explained 38% (partial correlation, R) of photoammonification rate (Table 3), whereas, pH explained 62%.

Discussion

Photoammonification in our study lakes converted only 0.18–0.3% of the DON pool to NH_3. This is considerably lower than rates of photoammonification observed in other studies. For example, previous studies have reported a conversion of 0.2–20% of the DON pool to NH_3 through photoammonification

Table 3 Multiple regression model for predicting photoammonification rate ($\log x + 1$) ($\mu g \, l^{-1} \, h^{-1}$) as a function of the logarithm of DON and/or dissolved organic carbon (DOC) concentration and pH. Results were derived using AIC to select the most parsimonious model among candidate model. Shown are the top two models selected by AIC

	Coefficient	SE	t Statistic	P value	Partial correlation (R)	ΔAIC
Top model						
$R^2 = 0.49$, $P < 0.001$, $n = 22$						
Intercept	−0.048	1.01	−0.047	0.96		0
Log DON ($\mu g \, l^{-1}$)	0.769	0.335	2.298	0.03	0.38	
pH	−0.232	0.061	−3.784	0.001	−0.62	
Second best model						
$R^2 = 0.51$, $P = 0.003$, $n = 22$						
Intercept	0.187	1.03	0.180	0.86		1.5
Log DON ($\mu g \, l^{-1}$)	0.886	0.355	2.497	0.02	0.51	
Log DOC ($\mu g \, l^{-1}$)	−0.346	0.347	−0.997	0.33	−0.23	
pH	−0.256	0.066	−3.887	0.001	−0.68	

(Bushaw et al., 1996; Bushaw-Newton & Moran, 1999; Wang et al., 2000).

A significant relationship between a300:DOC (or a350:DOC) and photoammonification rate was not observed in our study lakes. CDOM is preferentially lost (relative to DOC) during extended periods of solar irradiance (Moran et al., 2000) leading to the accumulation of more photo-refractory DOM with lower absorbance per unit carbon (c.f. Kitidis et al., 2006). Because of long water residence times, extensive photobleaching occurs in interior plains lakes (Art et al., 2000; Waiser & Robarts, 2000) and absorbance values tend to be low for a given DOC concentration (Table 1) (Sereda et al., 2011). For example, the a350:DOC values we report for our study lakes are much lower than a350:DOC values reported in other studies (see Table 2 this study, and Table 1 in Grzybowski, 2003). In turn, DOM in interior plain lakes may exhibit lower rates of photoammonification relative to lakes with more intensely colored DOC. Inclusion of lakes with greater chromophore content may be necessary to observe a relationship between DOM absorbance and photoammonification rates.

A significant relationship between pH and photo-ammonification rate was not observed in our study. This is in contrast to the observations of Wang et al. (2000) who reported that photoammonification rates increased $\sim$3-fold by lowering pH from 6 to $\sim$2. The increase in photoammonification with decreasing pH likely reflects enhanced hydroxyl radical production at lower pH accelerating the breakdown of DOM (Zepp et al., 1992). The pH in our study lakes had a narrow range of 7.9–8.7 (Table 1) and was likely too narrow to have observed a significant relationship between pH and photoammonification rate. However, in our subsequent analysis the range in pH was expanded (3.9–8.7) and pH was a significant predicator of photoammonification rate (Table 3).

Concentrations of ammonia did not increase in five of our study lakes following UVR treatment (Fig. 2). Three of these study lakes (Amisk, Bug, and Upper Blackstrap Lakes) were at the lower end of DON concentrations observed in our study lakes (Table 1). DON is a significant predictor of photoammonification (Table 3). Low DON concentrations may, in part, explain the lack of response in these lakes. However, two of our study lakes (Bradwell and Zelma) also did not respond to UVR treatment but had concentrations of DON greater than all of our other study lakes

(Table 1, Fig. 2). In systems with high ambient NH_3 concentrations the photochemically mediated loss of NH_3 may offset photoammonification (Koopmans & Bronk, 2002). Ambient concentrations of NH_3 in Bradwell and Zelma Lakes (mean = 215 μg NH_3 l^{-1}) were $\sim$17-fold greater than concentrations in our other study lakes (mean = 12.5 μg NH_3 l^{-1}). Photochemical loss of NH_3 in these systems may have off set photoammonification. Although, samples were sealed without head space to minimize NH_3 loss through volatilization, some NH_3 may have been lost through volatilization once samples were exposed to the atmosphere for analysis. A weak (non-significant) negative relationship between ambient NH_3 concentration and photoammonification was evident in our data. However, the relationship was largely influenced by the two extreme data points of Bradwell and Zelma. Koopmans & Bronk (2002) presented a relationship between ambient NH_4^+ concentrations and photoammonification. Their relationship encompassed a broader range in NH_4^+ concentration than our study lakes (5–30 μM or $\sim$70–420 μg l^{-1}). A net increase in NH_4^+ concentration was not observed at ambient NH_4^+ concentrations equal to or greater than $\sim$240 μg l^{-1} (Koopmans & Bronk, 2002). This concentration corresponds roughly with the ambient NH_3 concentrations in Bradwell and Zelma, and may represent a threshold concentration where photoammonification is offset by the photochemical-mediated loss of NH_3.

Our empirical model explained 49% of the variation in photoammonification rate across studies. The amount of variance explained by pH was greater than the variation explained by DON concentration (partial correlations of 0.62 and 0.38, respectively). This suggests that the rate of photoammonification is more dependent on pH than on substrate concentration. An increase in photo-product formation with decreasing pH is well documented. For example, the photoproduction of hydroxyl radicals (Zellner et al., 1990; Zepp et al., 1992), phosphate (Francko & Heath, 1982), Fe^{2+} (Emmenegger et al., 2001; Scully et al., 2003), and NH_3 (Wang et al., 2000) all increase as pH decreases. Product formation should increase with substrate concentration; however, substrate characteristics (e.g., chromophore content) should also influence rates of product formation. For example, increasing the chromophore content of DOM increases DOM UV absorptivity and photoreactivity (Bertilsson

& Tranvik, 2000; Lindell et al., 2000). Although we were unable to find a relationship between a300:DOC or a350:DOC and photoammonification in our study lakes, inclusion of absorbance ratios into the model from systems encompassing a greater range in CDOM concentration is likely to increase predictive power of the model.

In summary, this multi-lake study has illustrated that DON concentration and pH may be used to predict photoammonification rates. Photoammonification provides a new source of nutrients which can lead to an increase in primary production in N limited systems. Our photoammonification rates are lower than rates in other systems, and are likely a result of our study lakes being more alkaline with DON and CDOM concentrations generally lower than that of other studies. Future studies should focus on improving the predictive power of our model through inclusion of systems encompassing a broader range in CDOM concentration.

References

Art, M. T., R. D. Robarts, F. Kasai, M. J. Waiser, V. P. Tumber, A. J. Plante, H. Rai & H. J. de Lange, 2000. The attenuation of ultraviolet radiation in high dissolved organic carbon waters of wetlands and lakes on the northern Great Plains. Limnology and Oceanography 45: 292–299.

Arvola, L., 1981. Spectrophotometric determination of chlorophyll *a* and phaeopigments in ethanol extractions. Annales Botanici Fennici 18: 221–227.

Bachmann, R. & D. Canfield, 1996. Use of an alternative method for monitoring total nitrogen concentrations in Florida lakes. Hydrobiologia 323: 1–8.

Benner, R., 2002. Chemical composition and reactivity. In Hansell, D. A. & C. A. Carlson (eds), Biogeochemistry of Marine Dissolved Organic Matter. Academic Press, San Diego: 59–90.

Bergmann, M. & R. Peters, 1980. A simple reflectance method for the measurement of particulate pigment in lake water and its application to phosphorus–chlorophyll–seston relationships. Canadian Journal of Fisheries and Aquatic Sciences 37: 111–114.

Bertilsson, S. & L. J. Tranvik, 2000. Photochemical transformation of dissolved organic matter in lakes. Limnology and Oceanography 45: 753–762.

Bertilsson, S., R. Stepanauskas, R. Cuadros-Hansson, W. Granéli, J. Wikner & L. Tranvik, 1999. Photochemically induced changes in bioavailable carbon and nitrogen pools in a boreal watershed. Aquatic Microbial Ecology 19: 47–56.

Bronk, D. A. & B. B. Ward, 2002. Inorganic and organic nitrogen cycling in the Southern California Bight. Deep Sea Research Part I 52: 2285–2300.

Buffam, I. & K. McGlathery, 2003. Effect of ultraviolet light on dissolved nitrogen transformations in coastal lagoon water. Limnology and Oceanography 48: 723–734.

Burnham, K. P. & D. R. Anderson, 2004. Multimodel inference—understanding AIC and BIC in model selection. Sociological Methods & Research 33: 261–304.

Bushaw-Newton, K. & M. A. Moran, 1999. Photochemical formation of biologically available nitrogen from dissolved humic substances in coastal marine systems. Aquatic Microbial Ecology 18: 285–292.

Bushaw, K., R. Zepp, M. Tarr, D. Schulz-Jander, R. Bourbonniere, R. Hodson, W. Miller, D. Bronk & M. A. Moran, 1996. Photochemical release of biologically available nitrogen from aquatic dissolved organic matter. Nature 381: 404–407.

Crumpton, W., T. Isenhart & P. Mitchell, 1992. Nitrate and organic N analyses with second-derivative spectroscopy. Limnology and Oceanography 37: 907–913.

Emmenegger, L., R. R. Schonenberger, L. Sigg & B. Sulzberger, 2001. Light-induced redox cycling of iron in circumneutral lakes. Limnology and Oceanography 46: 49–61.

Francko, D. A. & R. T. Heath, 1982. UV-sensitive complex phosphorous: association with dissolved humic material and iron in a bog lake. Limnology and Oceanography 27: 564–569.

Gao, H. Z. & R. G. Zepp, 1998. Factors influencing photoreactions of dissolved organic matter in a coastal river of the southeastern United States. Environmental Science and Technology 32: 2940–2946.

Gardner, W., J. Cavaletto, H. Bootsma, P. Lavrentyev & F. Troncone, 1998. Nitrogen cycling rates and light effects in tropical Lake Maracaibo, Venezuela. Limnology and Oceanography 43: 1814–1825.

Grzybowski, W., 2002. The significance of dissolved organic matter photodegradation as a source of ammonium in natural waters. Oceanologia 44: 355–365.

Grzybowski, W., 2003. Are data on light-induced ammonium release from dissolved organic matter consistent? Chemosphere 52: 933–936.

Jørgensen, N. O. G., L. Tranvik, H. Edling, W. Granéli & M. Lindell, 1998. Effects of sunlight on occurrence and bacterial turnover of specific carbon and nitrogen compounds in lake water. FEMS Microbial Ecology 25: 217–227.

Kitidis, V., G. Uher, R. C. Upstill-Goddard, R. F. C. Matoura, G. Spyres & E. M. S. Woodward, 2006. Photochemical production of ammonium in the oligotrophic Cyprus Gyre (Eastern Mediterranean). Biogeosciences 3: 439–449.

Koopmans, D. J. & D. A. Bronk, 2002. Photochemical production of dissolved inorganic nitrogen and primary amines from dissolved organic nitrogen in waters of two estuaries and adjacent surficial groundwaters. Aquatic Microbial Ecology 26: 295–304.

Krupka, H. M., 1989. Transformations of nitrogen forms in epilimnion of the eutrophic Glebockie Lake (Masurian Lake District, Poland). Polskie Archiwum Hydrobiologii 36: 26–96.

Lindell, M. J., H. W. Graneli & S. Bertilsson, 2000. Seasonal photoreactivity of dissolved organic matter from lakes with

contrasting humic content. Canadian Journal of Fisheries and Aquatic Sciences 57: 875–885.

Moran, M. A., W. M. Sheldon & R. G. Zepp, 2000. Carbon loss and optical property changes during long-term photochemical and biological degradation of estuarine dissolved organic matter. Limnology and Oceanography 45: 1254–1264.

Morell, J. M. & J. E. Corredor, 2001. Photomineralization of fluorescent organic matter in the Orinoco River plume: estimation of ammonia release. Journal of Geophysical Research, Oceans 106: 807–813.

Prepas, E. E. & A. M. Trimbee, 1988. Evaluation of indicators of nitrogen limitation in deep prairie lakes with laboratory bioassays and limnocorrals. Hydrobiologia 159: 269–276.

Salm, C. R., J. E. Saros, S. C. Fritz, C. L. Osburn & D. M. Reineke, 2009. Phytoplankton productivity across prairie saline lakes of the Great Plains (USA): a step toward deciphering patterns through lake classification models. Canadian Journal of Fisheries and Aquatic Sciences 66: 1435–1448.

Sereda, J. M., D. M. Vandergucht & J. J. Hudson, 2011. Disruption of planktonic phosphorus cycling by ultraviolet radiation. Hydrobiologia 665: 205–217.

Scully, N. M., L. J. Tranvik & W. J. Cooper, 2003. Photochemical effects on the interaction of enzymes and dissolved organic matter in natural waters. Limnology and Oceanography 48: 1818–1824.

Stainton, M. P., M. J. Capel & F. A. J. Armstrong, 1974. The chemical analysis of fresh water. Fisheries Research Board of Canada 25: 35–37.

Stedmon, C. A., S. Markager, L. Tranvik, L. Kronberg, T. Slätis & W. Martinsen, 2007. Photochemical production of ammonium and transformation of dissolved organic matter in the Baltic Sea. Marine Chemistry 104: 227–240.

Stepanauskas, R., N. O. G. Jørgensen, O. R. Eigaard, A. Zvikas, L. Tranvik & L. Leonardson, 2002. Summer inputs of riverine nutrients to the Baltic Sea: bioavailability and eutrophication relevance. Ecological Monographs 72: 579–597.

Vahatalo, A. V., K. Salonen, U. Munster, M. Jarvinen & R. G. Wetzel, 2003. Photochemical transformation of allochthonous organic matter provides bioavailable nutrients in a humic lake. Archiv fur Hydrobiologie 156: 287–314.

Wang, W., M. A. Tarr, T. S. Bianchi & E. Engelhaupt, 2000. Ammonia photoproduction from aquatic humic and colloidal matter. Aquatic Geochemistry 6: 275–292.

Wiegner, T. N. & S. P. Seitzinger, 2001. Photochemical and microbial degradation of external dissolved organic matter inputs to rivers. Aquatic Microbial Ecology 24: 27–40.

Waiser, M. J. & R. D. Robarts, 2000. Changes in the composition and reactivity of allochthonous DOM in a prairie saline lake. Limnology and Oceanography 45: 763–774.

Wetzel, R. G., 2001. Limnology: lake and river ecosystems. Academic Press, San Diego.

White, E. M., P. P. Vaughan & R. G. Zepp, 2003. Role of the photo-Fenton reaction in the production of hydroxyl radicals and photobleaching of colored dissolved organic matter in a coastal river of the southeastern United States. Aquatic Sciences 65: 402–414.

Zar, J. H., 1999. Biostatistical Analysis. Prentice-Hall, London.

Zellner, R., M. Exner & H. Herrmann, 1990. Absolute OH quantum yields in the laser photolysis of nitrate, nitrite and dissolved H_2O_2 at 308 and 351 nm in the temperature-range 278–353 K. Journal of Atmospheric Chemistry 10: 411–425.

Zepp, R. G., B. C. Faust & J. Hoigne, 1992. Hydroxyl radical formation in aqueous reactions (pH 3–8) of iron(II) with hydrogen-peroxide—the photo-Fenton reaction. Environmental Science and Technology 26: 313–319.